



## Special Feature: Challenges of Internal Combustion Engines for Achieving Low-carbon Society

Research Report

### Verification of Thermo-swing Temperature Cyclic Fluctuation by Laser-induced Phosphorescence Thermometry

Kenji Fukui, Yoshifumi Wakisaka, Kazuaki Nishikawa, Yoshiaki Hattori, Hidemasa Kosaka and Akio Kawaguchi

Report received on Oct. 27, 2017

**■ABSTRACT■** This study aims to validate “thermo-swing” temperature fluctuations on the combustion chamber wall. The surface temperature of the thermo-swing insulation coating follows the gas temperature transiently. This reduces the temperature difference between the gas and the surface, causing a reduction in heat loss. To verify the swing phenomenon, we developed a technique to measure the temperature at a diesel spray flame impingement point, where a large heat loss reduction would be expected. The lifetime of laser-induced phosphorescence (LIP) was measured to determine the surface temperature, which has a high responsiveness. First, we confirmed that the sensitivity and response of this technique were sufficient for the investigation. Then, this technique was applied to a diesel spray flame impingement point. To reduce the occurrence of bright flames during optical measurements, we chose an oxygen-containing fuel in the place of normal diesel fuel. The temperature measurements of the insulation coating revealed a steep temperature rise during the combustion period and a temperature drop during the intake stroke. The swing width of the temperature in one cycle was approximately 140 K. On the other hand, the swing width with a non-insulation coating was about 45 K. The results showed a clear difference between the insulation and non-insulation coatings, which confirms the temperature swing phenomenon of the insulation coating. When these measured values were compared with the calculation results for one-dimensional heat conduction, the values were mostly consistent.

**■KEYWORDS■** Internal Combustion Engine, Temperature Measurement, Heat Insulation, Laser-induced Phosphorescence

#### 1. Introduction

To improve the thermal efficiency of an internal combustion engine and achieve a low-carbon society, ceramics have been applied to reduce the heat loss from the cylinders.<sup>(1,2)</sup> This approach focuses on the low thermal conductivity and high heat resistance of ceramics. However, because the heat capacity of ceramics is so large, the wall temperature increases through the whole engine cycle. This reduces the charging efficiency and causes knocking in gasoline engines. To overcome these problems, thermal insulation that does not raise the gas temperature during the intake stroke has been proposed.<sup>(3,4)</sup> To achieve this, we developed the “SiRPA” (silica-reinforced porous anodized aluminum) thermo-swing insulation coating, which has low thermal conductivity and low thermal capacity.<sup>(5-9)</sup> This reduces the heat flux from the

combustion chamber into the cooling water by making the wall temperature follow the gas temperature as much as possible during the expansion and exhaust strokes. During the intake and compression strokes, heating of the intake air is prevented because the wall temperature does not increase. The temperature cyclic fluctuation within a single cycle is referred to as the “temperature swing”.

Existing techniques to measure the surface temperature of the combustion chamber have used a thin-film thermocouple.<sup>(10-12)</sup> However, the heat capacity of thermocouple materials is not small enough relative to that of the insulation coating used in this study, which makes it difficult to measure the temperature swing with a thermocouple. There is also concern regarding the durability of a thermocouple junction and wire when it is installed on the moving parts of an engine. Thus, a noncontact measurement technique

has been developed whereby a radiation thermometer is used for the in-cylinder measurement.<sup>(13)</sup> To measure the temperature accurately, a blackbody spray should be applied to the surface of the object to be measured. There may be problems if a blackbody spray, which absorbs heat easily, is applied to an insulation coating with low thermal capacity. In this study, we focused on a temperature measurement technique that is based on the dependence of the phosphorescent lifetime on temperature. Although laser-induced phosphorescence (LIP) has already been applied to the surface of an engine combustion chamber,<sup>(14,15)</sup> this technique is limited to applications in which the temperature change within one cycle is small. In other words, a technique is needed for cases in which the surface temperature follows the gas temperature very responsively, as in the case of the newly developed SiRPA insulation coating. The area of greatest interest is near the diesel spray impingement point because the flow of the flame is intense, and a large heat loss reduction can be expected. However, optical temperature measurement methods that use phosphorescence have been reported as being difficult to apply because of the influence of the luminous flame.<sup>(16)</sup> In this study, we attempt to clarify the swing phenomenon at the spray impingement point.

We first confirmed the responsiveness of this measurement technique before applying the insulation coating. It proved possible to measure the temperature swing by reducing the effect of the luminous flame, which presents a problem during temperature measurement. Our results indicated that the temperature thermometry we developed demonstrated a swing phenomenon of 140 K for the SiRPA coating. For the base aluminum, however, the measured swing was only about 45 K. Therefore, a clear difference was confirmed in the swing phenomenon for these two cases.

## 2. Establishment of Laser-induced Phosphorescence Thermometry

### 2.1 Principle of Laser-induced Phosphorescence Thermometry

The lifetime of laser-induced phosphorescence (LIP) depends on temperature. This temperature dependence of phosphorescence has long been used to measure temperature in many fields.<sup>(17,18)</sup> Since the temperature

sensitivity differs depending on the phosphor, excitation wavelength, and observation wavelength, optimization of the combination of these parameters is important. The phosphor  $\text{La}_2\text{O}_2\text{S}:\text{Eu}$  has been reported to have a high temperature sensitivity in the range to be measured (approximately 373–573 K).<sup>(19)</sup> We selected an excitation wavelength of 355 nm and an observation wavelength of 620 nm.

### 2.2 Acquisition of Calibration Curves for the Temperature and Lifetime

We measured the phosphorescence lifetime  $\tau$  at different temperatures by changing the heater temperature, and then obtained a calibration curve using the polynomial approximation shown in **Fig 1**.

Phosphor was applied to the ceramic heater with a binder, and the signal from the phosphor was measured with a photomultiplier tube (PMT) through a bandpass filter. We measured the phosphorescence decay curve with an oscilloscope.

$$I(t)/I_0 = C \times \exp(-t/\tau) . \quad (1)$$

The phosphorescence intensity and decay waveform at time  $t$  can be approximated with Eq. (1) by using the initial intensity  $I_0$ , constant  $C$ , and lifetime  $\tau$ . Here, the initial intensity  $I_0$  was assumed to be the intensity after 10  $\mu\text{s}$  of laser incidence to reduce the effects of noise on the incident laser.

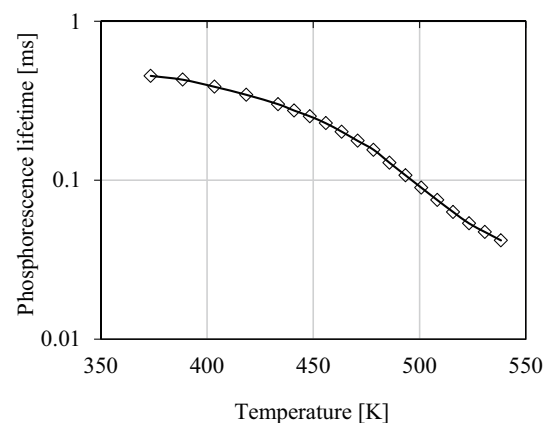


**Fig. 1** Calibration curve for temperature and lifetime.

### 2.3 Interface Between the Phosphor Film and Base Material

With this measurement method, we measured the surface temperature through the phosphor film attached to the object being measured. The phosphor was mixed with cellulose-based organic matter acting as a binder. It was then applied to the surface with an airbrush. The measured surface temperature of the phosphor must follow the surface temperature of the measurement object. Therefore, we observed the interface between the phosphor film and the surface by scanning electron microscopy (SEM). **Figure 2** shows an obtained SEM image. For these measurements, we observed a cross-section of the phosphor film. Although the phosphor particles were a few microns in diameter, we confirmed that they contacted the test pieces without any gap. Thus, we assumed that this represents an ideal state for measuring the surface temperature. The phosphor film should ideally be as thin as possible to reflect the surface temperature, but the signal-to-noise ratio (S/N) decreases for thinner films. Therefore, the thickness of the phosphor film was set to between 10 and 15  $\mu\text{m}$ . The influence of the film thickness on an engine will be described later.

### 2.4 Confirmation of the Transient Responsiveness

For the developed SiRPA coating, we estimated that there would be a rapid temperature rise upon spray flame collision. A temperature rise of 20 K or more in 1 ms during the combustion stroke was expected from the simulation results. Therefore, we checked the responsiveness of LIP thermometry before applying it to an engine. **Figure 3** shows the experimental

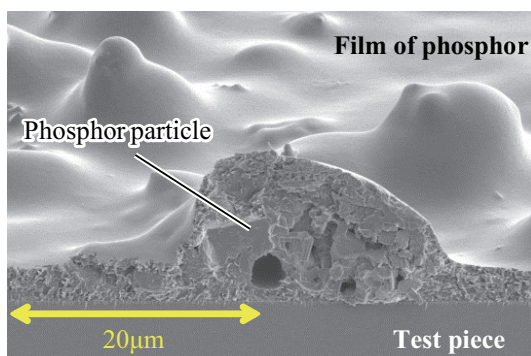


**Fig. 2** SEM image of phosphor film.

apparatus. Both sides of an aluminum foil of 20  $\mu\text{m}$  in thickness were coated with blackbody spray (emissivity: 0.94). A phosphor film was then applied on one side. By irradiating the back of the aluminum foil with focused light, a steep temperature rise could be attained. Prior to this, a halogen lamp was used to raise the surface temperature to at least 473 K before the pulsed laser irradiation. The temperature of the aluminum foil surface was measured with a radiation thermometer having a high temporal resolution (10  $\mu\text{s}$ ) and was obtained as the phosphorescence signals were being measured with the PMT. **Figure 4** shows the temperature results according to the LIP and the radiation thermometer. The horizontal axis shows the time after pulsed laser irradiation, and each measurement point was averaged to produce consistent

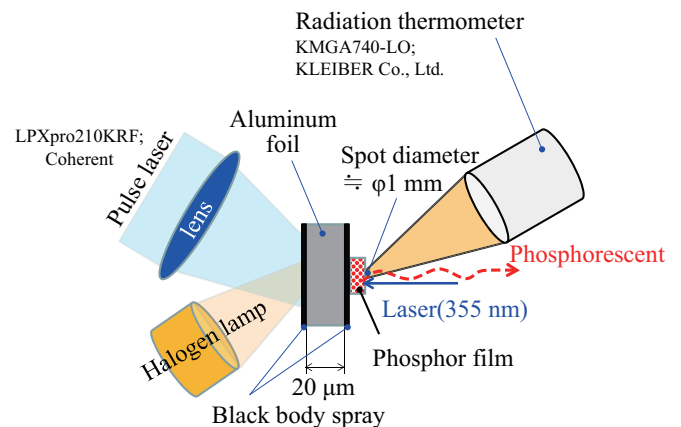


**Fig. 3** Experimental apparatus for confirming responsiveness.

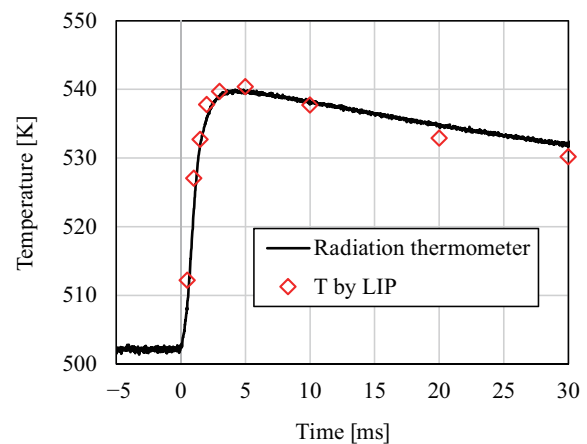


**Fig. 4** Temperature obtained by radiation thermometer and laser-induced phosphorescence.

time results. We confirmed the repeatability of the temperature rise of the aluminum foil using the radiation thermometer. The figure clearly confirms that the temperatures measured by the radiation thermometer and the phosphor were in good agreement. Because the emissivity of the surface of the blackbody spray ( $\epsilon = 0.94$ ) changed when the phosphor was applied, the emissivity of the radiation thermometer was set to 0.85 so that the temperatures would agree in the steady state. The rate of the temperature rise in this case was greater than or equal to 20 K/ms. Therefore, we confirmed that the temperature measurement technique using the phosphor can be applied to a temperature field with a rapid rise.

## 2.5 Specifications of the Optical Engine

**Table 1** lists the main specifications of the optically accessible engine<sup>(20)</sup> used in this experiment. **Figure 5** shows the experimental apparatus. The temperature

**Table 1** Engine specifications.

Engine	Optically accessible single-cylinder diesel engine
Displacement volume [cm <sup>3</sup> ]	557
Bore [mm] × Stroke [mm]	86 × 96
Compression ratio	15.83
Number of valve	Intake:2, Exhaust:1
Piston cavity shape	Bathtub type
Nozzle diameter × Hole number	φ0.09mm × 9holes

measurement point was in the vicinity of the spray flame impingement in the cavity on the piston surface. The pulsed laser irradiated the measurement point through a sapphire window mounted on the engine head side, while the phosphorescence signal was extracted coaxially. The measurement points are also shown in Fig. 5 ((a) aluminum, (b) SiRPA coating). The SiRPA insulation coating was formed on the aluminum piston. The physical properties of SiRPA will be described later herein (**Table 2**). A thermocouple was mounted to a depth of 200 μm on the piston (base aluminum material) to enable comparison of the temperature with that indicated by the phosphor.

## 2.6 Engine Operating Conditions for Removing the Luminous Flame

As mentioned in the introduction, removal of the luminous flame is important in LIP thermometry. The thermo-swing temperature fluctuation was measured at the spray flame impingement point because this was regarded as exhibiting a large reduction margin for the heat flux when the insulation coating was used. For this method, the phosphorescence signal at around 620 nm was measured. However, in this wavelength region, the broad spectrum of the luminous diesel flame is taken at the same time and superposed onto the signal from the phosphor. This was a major obstacle when measuring the temperature. Thus, the fuel was changed to diethylene glycol dimethyl ether (DGM), which has been reported to emit a smaller luminous flame than diesel fuel.<sup>(21)</sup> To confirm the brightness of the DGM flame,

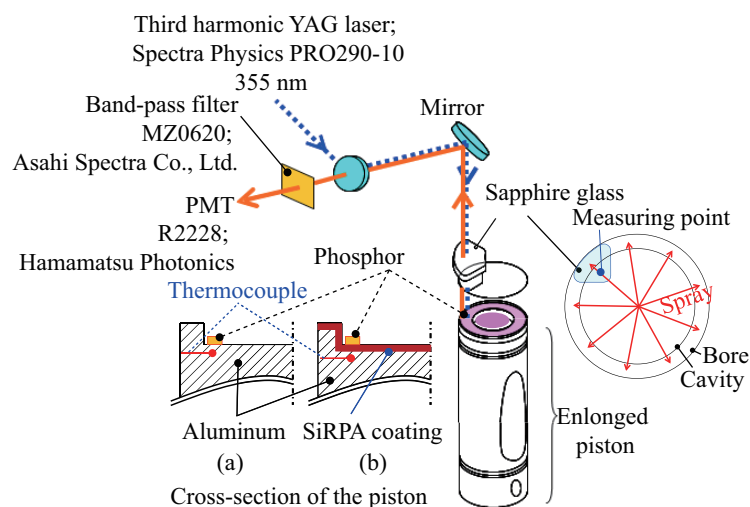


**Fig. 5** Experimental setup.

we captured combustion images with a high-speed camera (FASTCAM SA1.1; Photron Co., Ltd.) having a frame rate of 20000 fps. **Table 3** lists the experimental conditions. **Figure 6** shows the obtained results. The top of the figure shows typical images of the luminous flame, and the lower part shows the luminous flame brightness with respect to the crank angle. First, the brightness of the DGM in Case 1 was no more than 1/200 that of diesel fuel as determined with a simple brightness conversion. Note that the luminous flame of the diesel fuel image is omitted. The luminous flame brightness was defined as the average brightness of the images in grayscale. Case 1 had a highly luminous flame. In Case 2 (the injection pressure was raised and the oxygen concentration was reduced), the luminous flame was much smaller but still visible. Here, the oxygen concentration was adjusted by supplying  $N_2$  as a simulant EGR. To further reduce the intensity of the luminous flame, the oxygen concentration was reduced to 12%. Thus, a low-temperature combustion condition was realized in which almost no luminous flame was emitted (Case 3). **Figure 7** shows the phosphorescence signal

in Case 3, which was measured under motoring and firing conditions using the optical system. The crank angle in Fig. 7 was set to  $10^\circ$  after top dead center (ATDC) to compare the timing when the luminous flame was bright according to the visualization results. In motoring operation, only the base noise was observed. In firing operation, the luminous flame was superimposed on the base noise. The brightness of the luminous flame fluctuated with cycle variations, so this noise level was likely to change during the phosphorescence measurement.

If the luminous flame overlaps only in the initial phosphorescent stage, the slope of the decay increases, and the obtained phosphorescence lifetime is short. In this case, the temperature will be overestimated. Conversely, if the luminous flame overlaps only in the final phosphorescent stage, the slope of the decay decreases, and the phosphorescence lifetime is overestimated. In this case, the temperature will be underestimated. However, this noise level was sufficiently low compared with the intensity of the phosphorescence, so the error in the temperature calculation caused by the luminous flame was estimated to be about  $\pm 5$  K. The above results confirmed that we could measure the piston surface temperature at the instant of spray flame collision by using the oxygenated fuel and reducing the oxygen

**Table 2** Physical properties of aluminium and SiRPA coating.

	Aluminium	SiRPA coating	
		Case1	Case2
Thermal conductivity [W/mK]	125	0.65	1.4
Specific heat at constant volume [kJ/m <sup>3</sup> k]	2700	1624	2430
Density [kg/m <sup>3</sup> ]	2700	1500	2500
Thickness [ $\mu$ m]	—	100	

**Table 3** Combustion conditions.

	Case1	Case2	Case3
Engine speed	1200 rpm		
Fuel	DGM (Diethylene glycol dimethyl ether)		
Coolant temperature [ $^\circ$ C]	80		
Rail-pressure [Mpa]	60	80	
Pilot injection (timing [ $^\circ$ ATDC]/period [ms])	-20/0.26	-22/0.22	-20/0.24
Main injection (timing [ $^\circ$ ATDC]/period [ms])	-3/0.93	-3/0.6	-3/0.75
Injection quantity [mm <sup>3</sup> /st]	38.8	(unmeasured)	37.5
Oxygen concentration [%] ( $N_2$ diluted)	21.0	18.4	12.0

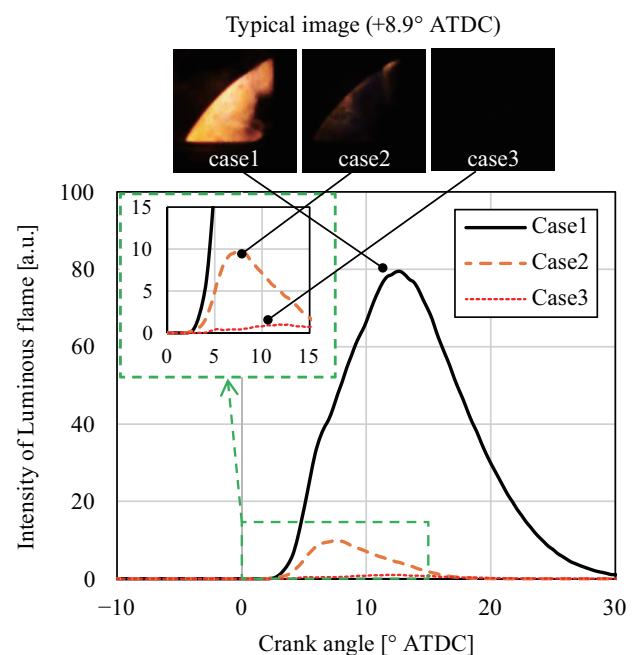


**Fig. 6** Brightness of luminous flame with respect to the crank angle.

concentration. Subsequent experiments addressing the temperature swing measurements were carried out under the same conditions as those described for Case 3. **Figure 8** shows the in-cylinder pressure and heat release rate under the combustion conditions. The combustion conditions used in this test were stabilized by pre-injection to promote the ignition of the main injections

### 3. Results

#### 3.1 Measurement Variations During Motoring Operation

The variation over 100 consecutive cycles during motoring operation was measured with an aluminum piston. The measured condition was in-cylinder pressure of 4.1 MPa at 15° ATDC. **Figure 9** shows the measurement temperature for the 100 consecutive cycles. The standard deviation of the measurement temperature was 3.8 K. During motoring operation, the temperature fluctuation was relatively small, and the measurement variation was about  $\pm 4$  K. Note that the temperature measured by the LIP was higher than that obtained by the thermocouple by about 7 K. This is considered to be caused by the fact that the thermocouple was positioned at a depth of 200  $\mu\text{m}$  from the surface.

#### 3.2 Influence of the Phosphor Film Thickness

The effects of the phosphor film thickness were evaluated with an aluminum piston. Two different

phosphor film thicknesses of about 10–15  $\mu\text{m}$  and 55–60  $\mu\text{m}$  were prepared. The film thickness was measured with a charge-coupled device (CCD) laser displacement meter (LK-G3000V; Keyence Corporation). **Figure 10** shows the temperature measurement results for a 5-s cycle before and after firing operation. The crank angle measured by LIP was fixed to 15° ATDC. The horizontal axis represents time. There were 30 cycles between 1 and 4 seconds during firing operation. The thermocouple measured the temperature of the metal part at a depth of 200  $\mu\text{m}$  from the surface, as shown in Fig. 5. When the operation switched from motoring to firing, the temperature rise was confirmed with the thermocouple on a cycle-by-cycle basis. According to LIP, the surface temperature changed suddenly before and after firing operation. From the Fig. 10, the temperature during the motoring period with the phosphor was equal to that obtained with the thermocouple for a phosphor thickness of 10–15  $\mu\text{m}$ . When the thickness was 55–60  $\mu\text{m}$ , however, the temperature was higher than that measured with the thermocouple. As the phosphor film thickness increased, the peak temperature became higher. **Figure 11** shows the mean and standard deviation of the temperature for each crank angle during the 30-cycle firing operation shown in Fig. 10 and the in-cylinder bulk gas temperature obtained from the gas state equation. For the thicker film case of 55–60  $\mu\text{m}$ , the peak temperature is higher than that of 10–15  $\mu\text{m}$  and the peak timing was delayed (10° ATDC for 10–15  $\mu\text{m}$ , 30° ATDC for 55–60  $\mu\text{m}$ ). This may be because the phosphor film itself functioned as an

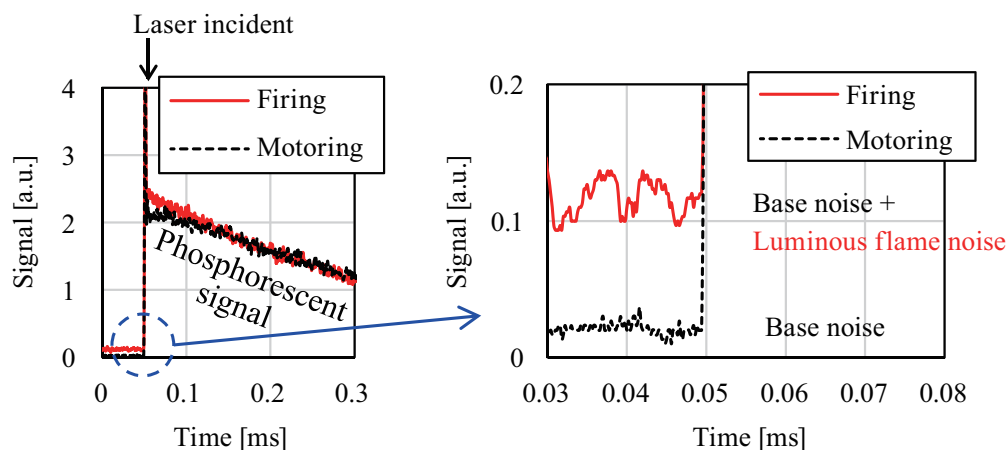


**Fig. 7** Influence of luminous flame on signal.

insulation coating. Although the bulk temperature decreases at +5° ATDC when the film thickness was 10–15 μm, the surface temperature also decreased. This indicates that the measured values for the phosphor temperature followed the gas temperature. Therefore, in order for the phosphor to follow the surface temperature, the film thickness of the phosphor needs to be reduced as much as possible. In this study, it proved difficult to reduce the thickness to 10 μm or less because of the low S/N ratio. Therefore, a phosphor film with a thickness of 10–15 μm was used in the following experiment.

### 3.3 Comparison of Aluminum and Insulation Coatings

As shown in Fig. 10, the thermocouple showed that the piston surface temperature continued to rise during firing operation. To suppress the influence of this temperature rise and the residual gas in the following experiments, the engine operating conditions were set to one firing operation per four cycles (skip firing), and the temperature was measured while the crank angle was shifted (e.g., -30° ATDC for the first firing, -20° for the second, -10° for the third, etc.). In this study, we used the SiRPA coating as insulation.

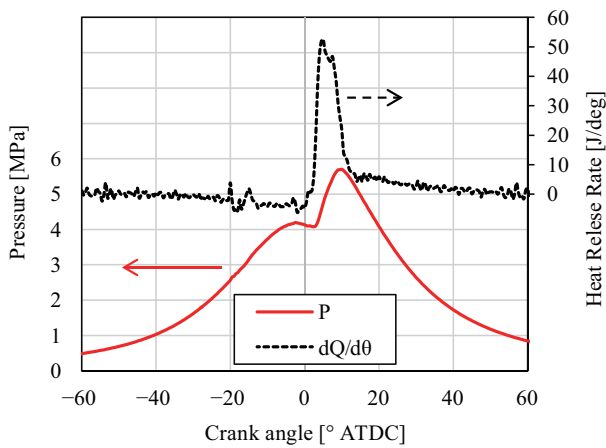


Fig. 8 Cylinder pressure and heat release rate.

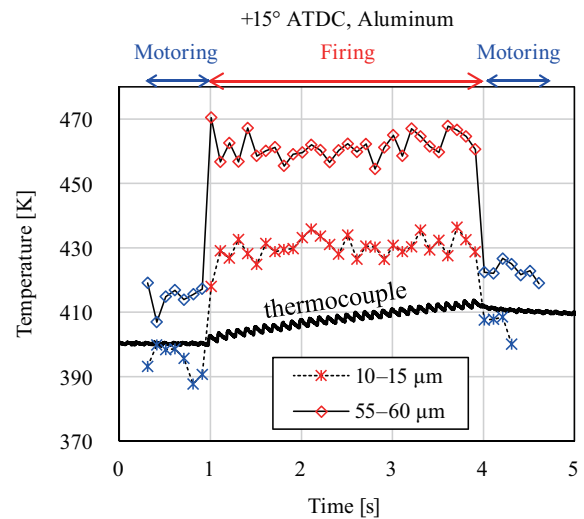


Fig. 10 Influence of the phosphor film thickness (time series).

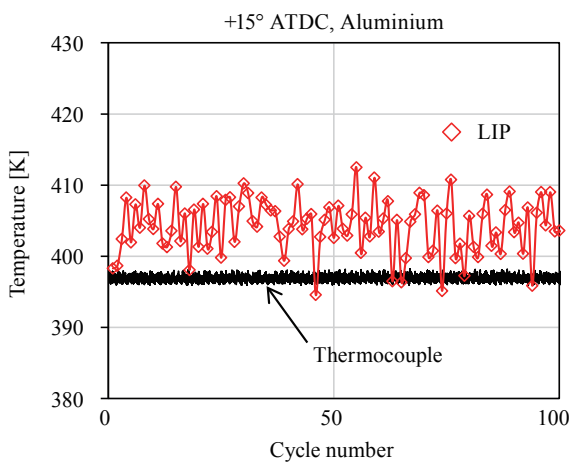


Fig. 9 Temperature measurement results (motoring conditions).

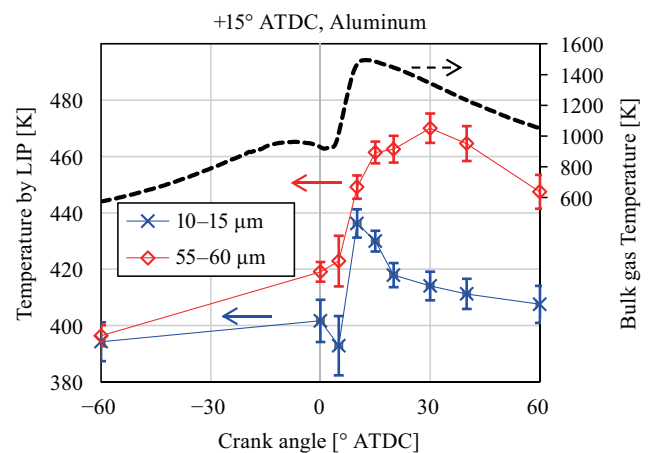
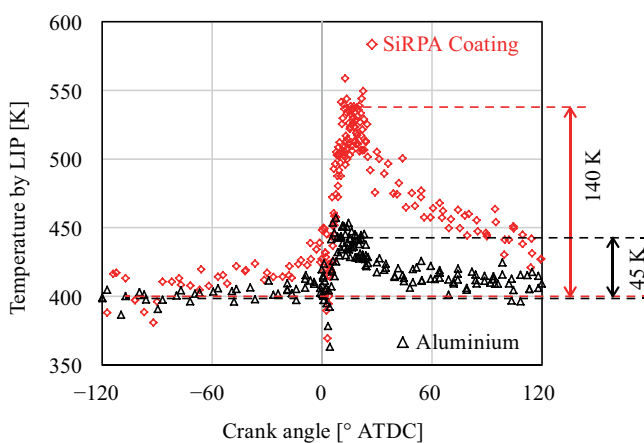


Fig. 11 Influence of the phosphor film thickness (average result).

is a porous alumina that can be formed by anodizing the cast aluminum alloy piston. Many pores with a size of several tens to several hundreds of nanometers are formed in the coating thickness direction. These pores contribute to the thermal insulation effect. The pores penetrate inwards from the surface. Thus, there is concern that the thermal insulation effect would be adversely affected if the high-temperature and high-pressure gas penetrates the inner membrane. Therefore, a silica coating of several microns in thickness was added to the porous alumina. Details of the insulation coating are given in Ref. 6. **Figure 12** shows the temperature measurement results under the base (aluminum) conditions and with the SiRPA coating. A steep temperature rise from near the TDC was confirmed for both the base aluminum and the SiRPA coating. For the SiRPA coating, a swing width of about 140 K or more was measured: 400 K for the intake stroke, and 540 K for the expansion stroke. On the other hand, a swing width of about 45 K was measured for the aluminum. Thus, a clear difference in the swing phenomenon for the two cases was confirmed. During the intake stroke, the temperature was almost the same for both cases, and there was no increase in the piston surface temperature. Therefore, as described in the introduction, there is no concern regarding a decrease in charging efficiency with this insulation coating. For both the aluminum base and SiRPA coating, the measurement variation was large at crank angles of 10°–30° ATDC. This large variation may mainly be caused by the flame behavior of the luminous flame in the cavity.



**Fig. 12** Result of temperature swing measurement.

#### 4. Comparison with the One-dimensional Heat Conduction Calculation

To validate the temperature swing phenomenon, the experimental results for the SiRPA coating, as shown in Fig. 12, were compared with the calculated results. We assumed an infinite flat plate to simulate the piston with an insulation coating formed on the flat plate. One-dimensional heat transfer calculations were performed for the wall in the vertical direction.<sup>(5)</sup> The heat transfer coefficient and the gas temperature obtained by a 3D computational fluid dynamics (CFD) simulation as a function of time were assigned at the temperature measurement position. The temperature at the rear of the piston was measured with the embedded thermocouple. Two cases describing the physical properties of the insulation coating were considered in order to estimate the density.

##### Case 1: Bulk density

The density was determined from the volume (with the open pore part being regarded as contributing to the volume), which was calculated from the dimensions and weight of the film.

##### Case 2: Apparent density

The density was determined from the volume (with the open pore part not being regarded as contributing to the volume), which was determined by the Archimedes method and the weight of the film.

Table 3 lists the respective physical properties of the aluminum and the SiRPA coating. **Figure 13** shows the measurement results (same as the results of the SiRPA coating shown in Fig. 12) and the calculated results. Generally, the calculated values tended to match the

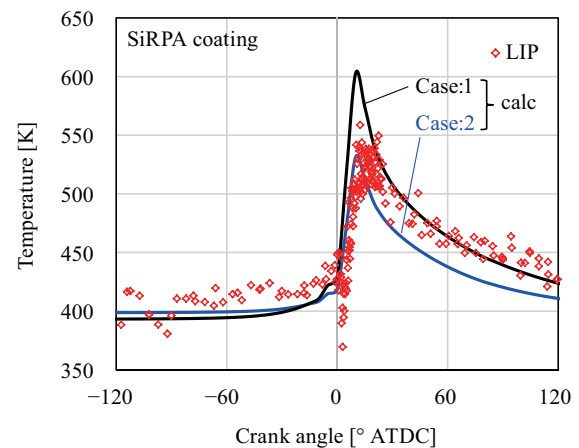


**Fig. 13** Experimental and calculation results.

measured values. The measurement results were close to Case 2 at the peak temperature and close to Case 1 when the temperature dropped during the expansion stroke. This suggests that gas may enter the insulation coating during the rapid pressure rise from combustion. Although the SiRPA coating was coated with silica, the gas seal may be incomplete. Based on these results, we can conclude that we can further enhance the heat insulation effect by improving the seal.

## 5. Conclusions

To verify the concept of a thermo-swing temperature coating that conforms to the gas temperature, we developed a temperature measurement technique based on the lifetime of laser-induced phosphorescence (LIP) for application to an optical engine, and obtained the following results.

- (i) The highly responsive temperature thermometry we developed demonstrated a swing phenomenon of 140 K for the SiRPA coating. For the base aluminum, however, the measured swing was only about 45 K. Therefore, a clear difference was confirmed in the swing phenomenon for the two cases.
- (ii) The temperature measurement technique based on the phosphor lifetime was confirmed to be highly responsive to temperature change, even with our developed insulation coating.
- (iii) To reduce the luminous flame, which is a problem with temperature measurements at the spray flame impingement point, where a large heat loss reduction can be expected as a result of adding the SiRPA coating, we changed the diesel fuel to oxygen-containing fuel (DGM) and decreased the in-cylinder oxygen concentration. In this way, we realized a combustion condition whereby almost no luminous flame is emitted.
- (iv) The temperature calculation error due to the luminous flame at the spray flame was no more than  $\pm 5$  K in this experiment.
- (v) The swing temperature width measured by LIP depended on the thickness of the phosphor. In this measurement, the thickness of the phosphor film was set to 10–15  $\mu\text{m}$ , and we reduced the swing effect of the phosphor itself.

## Acknowledgments

We are indebted to Dr. Tomoyuki Takada (Toyota Motor Corporation) for his valuable advice. We got cooperation from Dr. Kiyomi Nakakita and Dr. Yoshihiro Hotta through helpful discussion of the measurement results. We also received cooperation from Mr. Hiroaki Kadoura through the acquisition of SEM images.

## References

- (1) Bryzik, W. and Kamo, R., "TACOM/Cummins Adiabatic Engine Program", *SAE Tech. Pap. Ser.*, No. 830314 (1983).
- (2) Osawa, K., Kamo, R. and Valdmanis, E., "Performance of Thin Thermal Barrier Coating on Small Aluminum Block Diesel Engine", *SAE Tech. Pap. Ser.*, No. 910461 (1991).
- (3) Wong, V. W., Bauer, W., Kamo, R., Bryzik, W. and Reid, M., "Assessment of Thin Thermal Barrier Coatings for I.C. Engines", *SAE Tech. Pap. Ser.*, No. 950980 (1995).
- (4) Saad, D., Saad, P., Kamo, L., Mekari, M., Bryzik, W., Schwarz, E. and Tasdemir, J., "Thermal Barrier Coatings for High Output Turbocharged Diesel Engine", *SAE Tech. Pap. Ser.*, No. 2007-01-1442 (2007).
- (5) Kosaka, H., Wakisaka, Y., Nomura, Y., Hotta, Y., Koike, M., Nakakita, K. and Kawaguchi, A., "Concept of 'Temperature Swing Heat Insulation' in Combustion Chamber Walls, and Appropriate Thermo-physical Properties for Heat Insulation Coat", *SAE Int. J. Engines*, Vol. 6, No. 1 (2013), pp. 142-149.
- (6) Nishikawa, N., Takagishi, R., Shimizu, F. and Horie, T., "Heat Insulation by Temperature Swing in Combustion Chamber Walls (4th Report): Film for Temperature Swing Heat Insulation", *Proc. JSAE Annu. Congr.* (in Japanese), No. 6-15 (2015), pp. 166-171.
- (7) Wakisaka, Y., Inayoshi, M., Fukui, K., Kosaka, H., Hotta, Y., Kawaguchi, A. and Takada, N., "Reduction of Heat Loss and Improvement of Thermal Efficiency by Application of 'Temperature Swing' Insulation to Direct-injection Diesel Engines", *SAE Int. J. Engines*, Vol. 9, No. 3 (2016), pp. 1449-1459.
- (8) Fukui, K., Wakisaka, Y., Nishikawa, K., Hattori, Y., Kosaka, H. and Kawaguchi, A., "Development of Instantaneous Temperature Measurement Technique for Combustion Chamber Surface and Verification of Temperature Swing Concept", *SAE Tech. Pap. Ser.*, No. 2016-01-0675 (2016).

- (9) Kawaguchi, A., Iguma, H., Yamashita, H., Takada, N., Nishikawa, N., Yamashita, C., Wakisaka, Y. and Fukui, K., "Thermo-swing Wall Insulation Technology: A Novel Heat Loss Reduction Approach on Engine Combustion Chamber", *SAE Tech. Pap. Ser.*, No. 2016-01-2333 (2016).
- (10) Ishii, A., Nagano, H., Adachi, K., Kimura, S., Koike, M., Iida, N., Ishii, H. and Enomoto, Y., "Measurement of Instantaneous Heat Flux Flowing into Metallic and Ceramic Combustion Chamber Walls", *SAE Tech. Pap. Ser.*, No. 2000-01-1815 (2000).
- (11) Gralp, O., Hoffman, M., Assanis, D. N., Filipi, Z., Kuo, T.-W., Najt, P. and Rask, R., "Thermal Characterization of Combustion Chamber Deposits on the HCCI Engine Piston and Cylinder Head Using Instantaneous Temperature Measurements", *SAE Tech. Pap. Ser.*, No. 2009-01-0668 (2009).
- (12) Aoki, O., Tanaka, T., Nakao, Y., Kiyosue, R., Harada, Y. and Yamamoto, H., "Analysis of Heat Transfer Phenomena on High Response Heat Insulation Coatings by Instantaneous Heat Flux Measurement and Boundary Layer Visualization", *SAE Tech. Pap. Ser.*, No. 2015-01-1996 (2015).
- (13) Okabe, S., Morino, T., Hori, T. and Hanashi, K., "Spark Plug Temperature Measurement Using an IR Camera", *Denso Technical Review* (in Japanese), Vol. 13, No. 1 (2008), pp. 64-70.
- (14) Someya, S., Uchida, M., Tominaga, K., Terunuma, H., Yanrong, Li. and Okamoto, K., "Lifetime-based Phosphor Thermometry of an Optical Engine Using a High-speed CMOS Camera", *Int. J. Heat Mass Transfer*, Vol. 54, No. 17-18 (2011), pp. 3927-3932.
- (15) Srner, G., Richter, M., Aldn, M., Vressner, A. and Johansson, B., "Cycle Resolved Wall Temperature Measurements Using Laser-induced Phosphorescence in an HCCI Engine", *SAE Tech. Pap. Ser.*, No. 2005-01-3870 (2005).
- (16) Kashdan, J. and Bruneaux, G., "Laser-induced Phosphorescence Measurements of Combustion Chamber Surface Temperature on a Single-cylinder Diesel Engine", *SAE Tech. Pap. Ser.*, No. 2011-01-2049 (2011).
- (17) Noel, B. W., Borella, H. M., Franks, L. A., Marshall, B. R. and Allison, S. W., "Proposed Laser-induced Fluorescence Method for Remote Thermometry Inturbine Engines", *J. Propul. Power*, Vol. 2, No. 6 (1986), pp. 565-568.
- (18) Omrane, A., Juhlin, G., Ossler, F. and Aldn, M., "Temperature Measurements of Single Droplets by Use of Laser-induced Phosphorescence", *Appl. Opt.*, Vol. 43, No. 17 (2004), pp. 3523-3529.
- (19) Allison, S. W. and Gillies, G. T., "Remote Thermometry with Thermographic Phosphors: Instrumentation and Applications", *Rev. Sci. Instrum.*, Vol. 68, No. 7 (1997), pp. 2615-2650.
- (20) Fuyuto, T., Matsumoto, T., Hattori, Y., Kugimoto, K., Fujikawa, T., Akihama, K. and Ito, H., "A New Generation of Optically Accessible Single-cylinder Engines for High-speed and High-load Combustion Analysis", *SAE Int. J. Fuels Lubr.*, Vol. 5, No. 1 (2012), pp. 307-315.
- (21) Nabi, M., Minami, M., Ogawa, H. and Miyamoto, N., "Ultra Low Emission and High Performance Diesel Combustion with Highly Oxygenated Fuel", *SAE Tech. Pap. Ser.*, No. 2000-01-0231 (2000).

Figs. 1-13 and Tables 1-3

Reprinted from SAE Tech. Pap. Ser. No. 2016-01-0675 (2016), Fukui, K., Wakisaka, Y., Nishikawa, K., Hattori, Y., Kosaka, H. and Kawaguchi, A., Development of Instantaneous Temperature Measurement Technique for Combustion Chamber Surface and Verification of Temperature Swing Concept, © 2016 SAE International, with permission from SAE International.

**Kenji Fukui**

Research Fields:

- Laser Diagnostics
- Visualization of Combustion

Academic Societies:

- Society of Automotive Engineers of Japan
- The Japan Society of Mechanical Engineers

Awards:

- The Asahara Science Award, JSAE, 2009
- Outstanding Presentation Award, JSAE, 2015

**Hidemasa Kosaka**

Research Fields:

- Laser Diagnostics
- Gasoline/Diesel Combustion
- Engine System Simulation

Academic Society:

- Society of Automotive Engineers of Japan

Awards:

- The Asahara Science Award, JSAE, 2011
- The Outstanding Technical Paper Award, JSAE, 2015

**Yoshifumi Wakisaka**

Research Fields:

- Diesel Combustion
- Engine Heat Management

Academic Degree: Dr.Eng.

Academic Societies:

- The Japan Society of Mechanical Engineers
- Society of Automotive Engineers of Japan

Awards:

- The Ichimura Prize in Industry for Distinguished Achievement, The New Technology Development Foundation, 2017
- JSME Medal for New Technology, 2017
- The Outstanding Technical Paper Award, JSAE, 2017
- The Technological Development Award, JSAE, 2017

**Akio Kawaguchi\*\***

Research Field:

- Thermal Efficiency Improvement of Internal Combustion Engines

Academic Societies:

- Society of Automotive Engineers of Japan
- The Japan Society of Mechanical Engineers

Awards:

- The Outstanding Technical Paper Award, JSAE, 2013, 2017
- R&D 100 Awards, 2016
- JSME Medal for New Technology, 2017
- The Ichimura Prize in Industry for Distinguished Achievement, The New Technology Development Foundation, 2017
- The Technological Development Award, JSAE, 2017

**Kazuaki Nishikawa**

Research Field:

- Engine Combustion



\*Toyota Motor Corporation

**Yoshiaki Hattori**

Research Field:

- Engine Combustion

Award:

- The Outstanding Technical Paper Award, JSAE, 1997 and 2013

